NANO LETTERS

pubs.acs.org/NanoLett Letter

Formation of Defects in Two-Dimensional MoS_2 in the Transmission Electron Microscope at Electron Energies below the Knock-on Threshold: The Role of Electronic Excitations

Silvan Kretschmer,*[,‖] Tibor Lehnert,[‖] Ute Kaiser, and Arkady V. Krasheninnikov

Cite This: *Nano Lett.* 2020, 20, 2865−2870 Read Online

ACCESS | Metrics & More | Article Recommendations | Supporting Information

ABSTRACT: Production of defects under electron irradiation in a transmission electron microscope (TEM) due to inelastic effects has been reported for various materials, but the microscopic mechanism of damage development in periodic solids through this channel is not fully understood. We employ non-adiabatic Ehrenfest, along with constrained density functional theory molecular dynamics, and simulate defect production in two-dimensional MoS_2 under electron beam. We show that when excitations are present in the electronic system, formation of vacancies through ballistic energy transfer is possible at electron energies which are much lower than the knock-on threshold for the ground state. We further carry out TEM experiments on single layers of MoS_2 at electron voltages in the range of 20−80 kV and demonstrate that indeed there is an additional channel for defect production. The mechanism involving a combination of the knock-on damage and electronic excitations we propose is relevant to other bulk and nanostructured semiconducting materials.

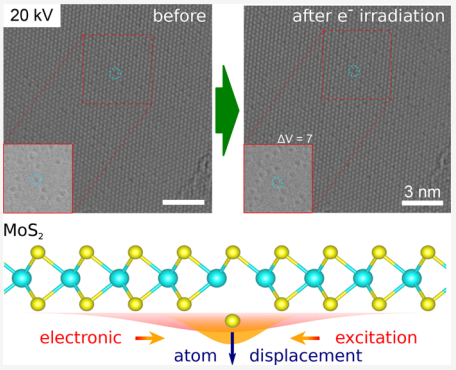

KEYWORDS: *Two-dimensional materials, transition-metal dichalcogenides, high-resolution transmission electron microscopy, defects*

The particle-wave dualism, as postulated by de Broglie,[1] is one of the fundamental concepts in physics directly relevant to transmission electron microscopy (TEM). The formation of the TEM image can be understood in terms of the interference of electrons which passed through a thin specimen, while momentum transfer to its atoms and electrons from the impinging high-energy electrons is most intuitively described in the particle picture. The latter process can give rise to defect production in the specimen and normally needs to be avoided to get the information about its atomic structure without modifying or even destroying it completely. The solution to this problem requires a detailed understanding of the damage formation by high-energy electrons. Three mechanisms (see refs 2−5 for an overview) can contribute to the defect production: (i) the knock-on damage[6,7] due to elastic electron scattering and direct momentum transfer from the electron to a target atom, (ii) damage due to inelastic electron scattering and energy transfer to the electronic system of the semiconducting and insulating target material leading to electronic excitation and electrostatic charging[6,8] (radiolysis), and (iii) beam-induced chemical etching.[9,10] The first channel normally dominates at high electron voltages, but it is expected to be inactive at voltages below a certain value, the so-called knock-on threshold U_{th}, as the electron is not able to transfer enough kinetic energy to the recoil atom and displace it. Thus, avoiding knock-on damage has been the driving force behind decreasing the voltage at which a TEM operates,[11,12] especially after the development of aberration correctors.[12−16]

The emergence of two-dimensional (2D) materials[17] attracted additional attention to the damage problem, as many of these systems proved to be radiation-sensitive materials.[2,18] At the same time, their very geometry, which enables one to identify single atoms, made it possible to quantify the damage at different voltages by directly counting missing atoms[9,19] and imaging the development of the damage in the specimen with atomic resolution.[20−23] Nevertheless, the defect production channels mentioned above are difficult to differentiate,[2] and the role of electronic excitations is not well understood. Currently, there is no quantitative microscopic theory describing the relation between the amount of energy deposited in the specimen through electronic excitations and damage creation in periodic solids. The lifetime of a core hole in inorganic 2D materials (of the order of a few fs)[2,24] is too short as compared to the time required to break a bond by displacing an atom (~10^2 fs) so that core holes alone can hardly give rise to damage formation. The core hole can be converted to valence electron excitation through Auger processes with a much longer lifetime (~10^6 fs)[2] in

Received: February 15, 2020
Revised: March 16, 2020
Published: March 20, 2020

https://dx.doi.org/10.1021/acs.nanolett.0c00670
Nano Lett. 2020, 20, 2865−2870

semiconducting and insulating materials, but the simplistic picture that excited electrons in materials in antibonding states cause the bonds to break is misleading for crystalline materials under electron beam in the TEM, as very few electrons are excited (the deposited energy is many orders of magnitude smaller than that under laser irradiation when it gives rise to structural changes in inorganic 2D materials, see Supporting Information (SI) for the estimates), and, contrary to amorphous materials, isolated molecules, or bulk molecular crystals, there is no physical reason why the excitation should be localized on a particular bond. At the same time, numerous experiments indicate that defects are produced in inorganic 2D materials at voltages (e.g., 60 kV)[20,21] well below $U_{th} \sim 80$ kV.[7,25]

Here, using first-principles simulations, we study the production of defects in 2D MoS_2 at voltages below U_{th} and suggest a mechanism which can be responsible production. Specifically, we show that when the electronic system of the specimen is in the excited state, the excitation can localize on the emerging defect, which gives rise to the substantial drop in the displacement threshold energy, so that formation of vacancies at electron voltages well below U_{th} is possible. We further carry out TEM experiments where we directly assess the amount of damage created by the beam experimental data.

To assess the combined effect of electronic excitations and ballistic energy transfer from the impinging electrons to the recoil atoms, we carried out atomistic density functional theory (DFT) simulations. We used several computational approaches. Specifically, we employed the non-adiabatic Ehrenfest dynamics (ED) based on time-dependent DFT as implemented in the GPAW code.[26] Although ED, as a mean-field approach, in which the nuclei evolve in an effective time-dependent electronic potential in a state mixture, has several shortcomings,[27] it has provided lots of insight into fast processes in solids, for example, stopping of energetic particles in materials[28−30] or excitation-mediated diffusion.[31]

In the second set of simulations, we assessed the displacement threshold T_d, that is the minimum kinetic energy which must be assigned to the recoil atom to displace it without immediate recombination with the vacancy, in the presence of excitations using constrained DFT molecular dynamic (c-DFT MD) simulations with the PBE exchange−correlation functional[32] and the projector augmented wave (PAW) formalism[33] as implemented in the VASP code.[34,35] Here the excitation was modeled by keeping the occupancies of the states at valence band maximum (VBM) and conduction band minimum (CBM) fixed. The details of simulations are given in SI.

We started by carrying out ED simulations of a 40 keV electron impinging on 2D MoS_2, see Figure 1. The electron in these simulations was modeled as a classical point particle with the mass of an electron, negative charge, and the interaction with the electron/nuclei described by a modified hydrogen PAW potential. The details are given in SI. This approximation is justified by the small ($\sim 10^{-2}$ Å) de Broglie wavelength of the energetic electrons in the TEM, and it is close to the approach where the energetic electron is approximated as a point source electric field impulse.[36,37] We stress that such an approximation cannot be used to model electron scattering or formation of the TEM images. The simulations indicate that the electron transfers a part of its kinetic energy to the electronic system of the target and leaves the system in a state mixture comprising a valence band excitation. The excitation is

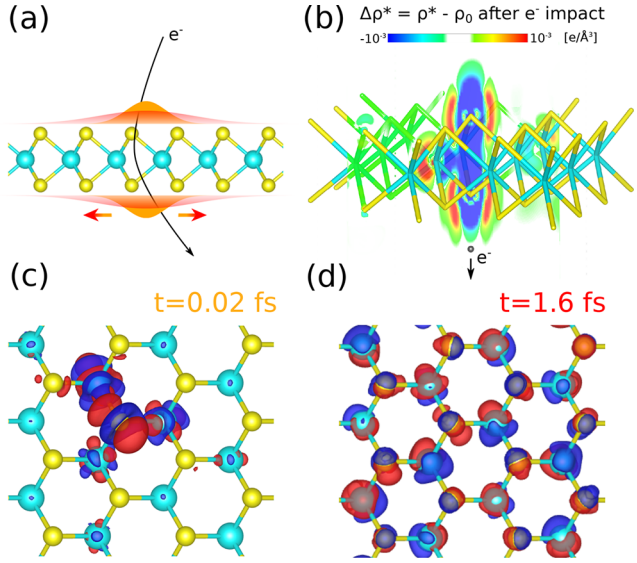

Figure 1. ED simulations of a high-energy electron impact into a MoS_2 sheet. The electron is modeled as a classical particle with a precisely defined trajectory, which can give rise to electronic excitations in the target material, as schematically illustrated in (a). (b) The spatial extent of the electronic excitation created in the system immediately after the impact. (c) Simulations where exactly one electron is excited with the excitation initially being localized on a sulfur atom. (d) The spatial extent of the excitation after 1.6 fs as described within the framework of ED.

initially localized (Figure 1b), but it is spread over the whole system after a few fs. The energy deposition is rather small in this approach, as the PAW potential is too "soft" at small distances from the particle.

In order to investigate the time evolution of the excitation further and also account for a stronger perturbation of the electronic system by the electron impact, a separate set of ED simulations was performed. Exactly one electron was excited into the CBM with a localization length of about 1 Å (Figure 1c). Further details can be found in SI. The charge density difference for the excited state $\Delta\rho^*(t) = \rho^*(t) - \rho_0(t)$, where ρ^* and ρ_0 are the charge densities of the excited state and the ground state for a given atom configuration, respectively, was evaluated as a function of time t. The evolution of $\Delta\rho^*(t)$ initially centered at a sulfur atom shows that the excitation will spread over the pristine lattice on a fs time-scale (Figure 1d), similar to what was observed in the first simulation setup. This confirms that in the pristine system, there is no physical reason why the excited electron should be localized on a particular bond when all the atoms are equivalent.

The behavior of the system is, however, completely different when the translation symmetry is broken, for example, by an emerging defect. Physically, this is the situation when an electron ballistically transfers some energy to the recoil atom and, at the same time, gives rise to electronic excitation (or the excitation pre-existed in the system), as schematically shown in Figure 2a. As we demonstrated previously, the delocalization time of the excitation is very short, so that it is not important for the evolution of the atomic system if the excitation was initially localized on the recoil atom or a few Å away. To address this, we carried out another set of simulations, where a delocalized electronic excitation was created, and, at the same time, kinetic energy of 7.0 eV was assigned to one of S atoms. The evolution of $\Delta\rho^*(t)$ in Figure 2b shows the localization of

https://dx.doi.org/10.1021/acs.nanolett.0c00670
Nano Lett. 2020, 20, 2865−2870

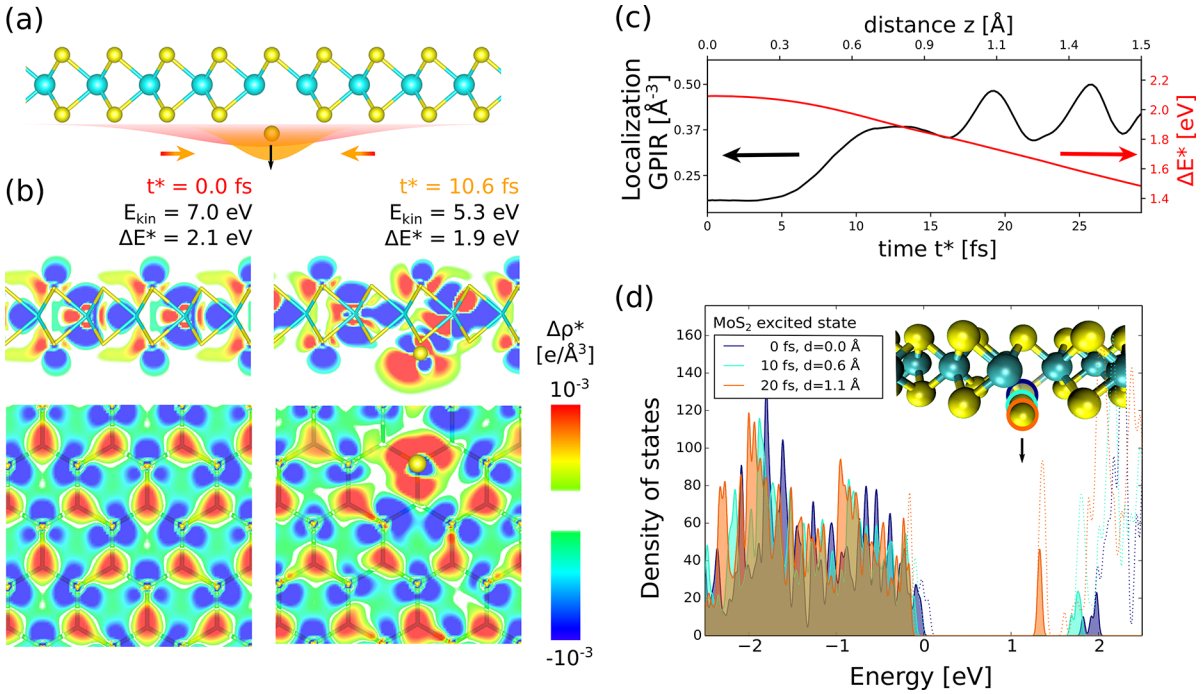

Figure 2. (a) Sketch of the initial simulation ED setup with a delocalized excitation, which localizes at the incipient vacancy when initial kinetic energy is assigned to the recoil S atom. (b) Evolution of the excitation in MoS_2 sheet, side and top views, which localizes at the emerging vacancy, as quantified in panel (c), that also shows the change in the energy of the recoil atom. excitation energy. (d) The static electronic structure of MoS_2 sheet with emerging S vacancy for several positions of the recoil atom with d being its displacement from the original position, as calculated by c-DFT. The occupied defect state localized at the vacancy splits off from the CBM.

the excitation at the emerging vacancy site. The charge density difference can be analyzed in more detail by calculating the generalized inverse participation ratio (GIPR)[38] for $\Delta\rho^*$ defined as

$$\mathrm{GIPR}(t) = \int |\Delta\rho^*(\vec{r}, t)|^2 \, dV \Big/ \left[\int |\Delta\rho^*| dV\right]^2 \quad (1)$$

As evident from Figure 2c, localization of $\Delta\rho^*$ is substantial after 10 fs, when the recoil S atom is displaced by more than 0.6 Å. A decrease in the energy difference $\Delta E^* = E^* - E_0$, where E^* and E_0 are the excited- and ground-state energies, is related to the displacement of the atom, accompanied by the appearance of a defect state in the band gap of the material as the S atom moves out-of-plane. This is confirmed by static calculations of the density of states at different times during the displacement process shown in Figure 2d. As ED simulations are computationally too expensive to calculate T_d, we used c-DFT MD to assess it. The initial kinetic energy was varied in order to find T_d. An atom in the simulations was considered to be displaced when it moved at least 4.5 Å from its initial position and it has a velocity component still pointing away from the MoS_2 sheet. Additionally, it was checked that the average force on the recoil atom is below 0.01 eV/Å. This situation is typically achieved for simulation times of about 400−600 fs (time step 0.2 fs). The conditions imposed on the recoil atom ensure that it will not come immediately back and fill the defect site.

The results are summarized in Table 1. For nonspin-polarized calculations, T_d for the ground state was found to be 7.1 eV in agreement with previous calculations.[7] We also repeated calculations with account for spin-polarization and expectedly received lower values for T_d (by spin-polarization energy of an isolated atom). We stress, though, that the ground-state DFT MD cannot adequately describe the dynamics of the system associated with a spin flip, so that we list both non- and spin-polarized values. Table 1 also gives T_d when a core hole with an infinite lifetime is present at the recoil S atom. The details of simulations are given in SI. T_d also dramatically decreases, but as the actual lifetime of core holes is very short, just a few fs, as discussed above, this process cannot govern defect production, although it may still contribute to the creation of defects at the early stages of duamage development, effectively lowering T_d.

Table 1. Displacement Thresholds T_d and Corresponding (Static) Electron Voltage U_{th} for S Atom in 2D MoS_2 without and with Account for Spin-Polarization

	nonspin-polarized		spin-polarized	
	T_d (eV)	U_{th} (kV)	T_d (eV)	U_{th} (kV)
ground state	7.1	95.4	6.5	87.9
1× excited e^-	5.3	72.7	4.8	66.2
2× excited e^-	3.75	52.4	3.5	49.1
core hole			2.4	34.1

In the same simulation setup, we found a pronounced drop in the threshold to 4.8 eV, when one electron was in the excited state. T_d decreases further to 3.5 eV for the double excitation. This illustrates that initially delocalized electronic excitations localize on the incipient vacancy and have a dramatic effect on the behavior of the system when kinetic energy is transferred to one of the atoms.

Since displacement cross section data are available mostly for high (above 60 kV) voltages,[7,39] we performed measurements of this quantity by directly analyzing high-resolution (HR)TEM images of MoS_2 sheet obtained at voltages below U_{th}. Figure 3a presents Cc/Cs-corrected HRTEM images of

https://dx.doi.org/10.1021/acs.nanolett.0c00670
Nano Lett. 2020, 20, 2865−2870

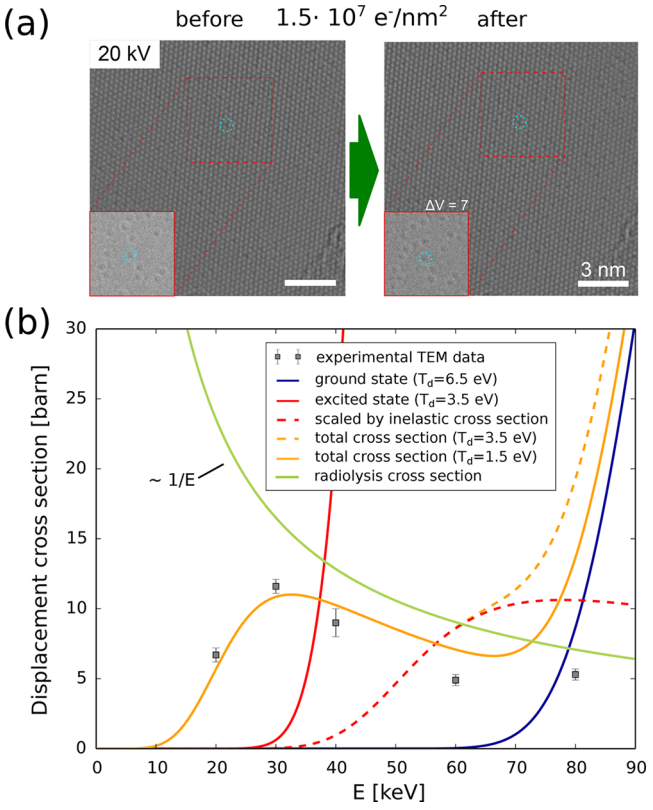

Figure 3. (a) Cc/Cs-corrected HRTEM images of single-layer MoS_2 before and after exposure to the total dose of 1.5×10^7 electrons/nm^2 at an acceleration voltage of 20 kV. During irradiation, S vacancies appear. Fourier-filtered images from the red dashed framed area are given in the insets (solid frames). As an example, a vacancy in each filtered and raw image is marked by a cyan circle. ΔV gives the number of the produced vacancies. (b) The experimental (squares) and theoretical (curves) displacement cross sections σ of S atoms in MoS_2, as calculated within the framework of the McKinley−Feshbach formalism with account for thermal vibrations and with different values of displacement threshold T_d, corresponding to the ground and excited states. The decrease in the excitation probability with increasing electron energy is accounted for within the framework of the Bethe theory. The total cross section with a T_d = 1.5 eV, which matches the experimental data reasonably well, is also shown.

single-layer MoS_2 obtained at 20 kV before and after exposure to the total dose of 1.5×10^7 electrons/nm^2. The HRTEM images were aqcuired with a dose rate of 6.7×10^5 electrons/(nm^{2}s). Similar images obtained at other voltages (20, 30, 40, 60, and 80 kV) are shown in SI. For easier identification of the vacancies, the images were Fourier filtered to remove the MoS_2 lattice. The insets in the panels show such images (solid frames) from the dashed framed areas. It is evident from the TEM images that vacancy concentration increases over time. For quantitative evaluation, the displacement cross-section σ was determined as $\Delta V/(N\phi)$. ΔV is the number of produced vacancies after an accumulated dose ϕ in an area with N sulfur atoms. Values for ΔV are also given in SI.

The experimental values of σ are summarized in Figure 3b. A notable feature is a smaller value of σ at 20 keV as compared to that at higher energies, which indicates that there is a channel for defect production with threshold energy well below the ground-state T_d. Neither the excitations alone nor chemical etching (associated predominantly with the creation of reactive species by removing H atoms from water molecules) can be responsible for damage production at low voltages, as the effectiveness of both processes monotonously decreases with voltage. We stress that σ increases fast at voltages above 80 kV, and it is of the order of 10^2 barn at 200 kV.[39]

The McKinley−Feshbach formalism[40] with account for thermal vibrations[9] allows to evaluate σ using the calculated T_d and compare it to the experimental values. The total cross section $\sigma^{tot}(E)$ will be a sum of the two needed cross sections which include knock-on events for the ground $\sigma(E,T_d^{gs})$ and excited $\sigma(E,T_d^{exc})$ states:

$$\sigma^{tot}(E) = \sigma(E, T_d^{gs}) + \sigma(E, T_d^{exc}) \times \chi_{inel}^{Bethe}(E) \quad (2)$$

with the latter being scaled by the probability $\chi_{inel}^{Bethe}(E) \sim 1/E$,[41,42] to excite target electrons as a function of impinging electron energy E, see SI for detail.

Figure 3b shows σ for the valence band excitations (T_d^{exc} = 3.5 eV, red curve) and the ground state (T_d^{gs} = 6.5 eV, blue), along with $\chi_{inel}^{Bethe}(E)$. The values of T_d are taken from Table 1. As χ_{inel}^{Bethe} decreases with E, one can expect that $\sigma^{tot}(E)$ can qualitatively describe the trends in the experimental observations. However, as evident from the dashed curves in Figure 3b, the decrease in the radiolysis cross section is not fast enough to provide a minimum on the total cross section curve. For the quantitative agreement, T_d^{exc} should be lower than the calculated value, with the best fit yielding T_d^{exc} = 1.5 eV, yellow solid line. The lowering of the effective displacement threshold may be related to the contribution from core holes at the initial stages of damage development or multielectron excitations.

The excitation can hypothetically be created by not only that same electron which displaces the atom but also by another electron. The lifetime of an excitation in a MoS_2 is about 1 ps,[43,44] order of magnitude as the average time between two consecutive impacts of electrons into an area with dimensions of about 10 × 10 nm^2 for the high current densities of 10^5−10^6 A/cm^2. This is considerably higher than what can be achieved in our experimental setup, but in thicker specimens (the probability to excite electrons should be proportional to the thickness of the target) with a long excitation lifetime, a two-electron process may be possible: An electron creates an excitation which is delocalized in the system and persists long enough for another electron to hit a nearby region and move the recoil atom from its position in the pristine lattice. The breakup of the translational symmetry, in turn, leads to the localization of the excitation at the emerging vacancy site, lowering the binding energy and therefore the displacement threshold. This indicates that the defect production rate (per number of impinging electron) should be higher at high beam currents, which has indeed been found in the experiments on the inorganic materials[3] for which radiolysis is the main channel for defect production.

To sum up, using non-adiabatic ED combined with TD-DFT, along with constrained DFT MD, we showed that formation of vacancies in a single sheet of MoS_2 is possible at electron voltages well below the knock-on threshold due to the combined effect of electronic excitations and knock-on damage. We demonstrated that when a delocalized electronic excitation exists in a semiconducting material, it can localize on the emerging defect, for example, incipient vacancy at the position of the recoil atom created by ballistic energy transfer from the impinging energetic electron, weakening the local chemical bonds. This leads to another channel for defect production with a much lower threshold energy. The results of

https://dx.doi.org/10.1021/acs.nanolett.0c00670
Nano Lett. 2020, 20, 2865−2870

our TEM experiments on single-layer MoS_2 sheets at electron voltages in the range of 20−80 kV are consistent with that picture. The mechanism we propose is relevant to other semiconducting materials and, in addition to beam-induced chemical etching, can be responsible for damage production in a wide range of materials at low electron voltages.

■ ASSOCIATED CONTENT

Supporting Information

The Supporting Information is available free of charge at https://pubs.acs.org/doi/10.1021/acs.nanolett.0c00670.

Details of calculations and TEM experiments, along with additional TEM images of MoS_2 sheets before and after exposure to the electron beam. The estimates of energy deposition under typical imaging conditions in TEM experiments are also presented (PDF)

■ AUTHOR INFORMATION

Corresponding Author

Silvan Kretschmer − *Institute of Ion Beam Physics and Materials Research, Helmholtz-Zentrum Dresden-Rossendorf, 01328 Dresden, Germany;* orcid.org/0000-0002-5098-5763; Email: s.kretschmer@hzdr.de

Authors

Tibor Lehnert − *Central Facility for Electron Microscopy, Group of Electron Microscopy of Materials Science, Ulm University, Ulm 89081, Germany;* orcid.org/0000-0002-4904-9580

Ute Kaiser − *Central Facility for Electron Microscopy, Group of Electron Microscopy of Materials Science, Ulm University, Ulm 89081, Germany*

Arkady V. Krasheninnikov − *Institute of Ion Beam Physics and Materials Research, Helmholtz-Zentrum Dresden-Rossendorf, 01328 Dresden, Germany; Department of Applied Physics, Aalto University, 00076 Aalto, Finland;* orcid.org/0000-0003-0074-7588

Complete contact information is available at: https://pubs.acs.org/10.1021/acs.nanolett.0c00670

Author Contributions

‖Contributed equally to this work

Notes

The authors declare no competing financial interest.

■ ACKNOWLEDGMENTS

We thank K. Suenaga, J. Meyer, J. Kotakoski, T. Susi, R. Egerton, and A. Schleife for discussions. We acknowledge funding from the German Research Foundation (DFG), project KR 48661/1. T.L. and U.K. further acknowledge financial support by the EU within the Graphene Flagship and by the DFG in the frame of the *SALVE* project as well the Ministry of Science, Research. and Arts (MWK) of Baden-Wuerttemberg. The further thank CSC Finland, HLRS, Stuttgart, Germany, and TU Dresden (Taurus cluster) for generous grants of CPU time.

■ REFERENCES

(1) de Broglie, L. Recherches sur la théorie des Quanta. *Ann. Phys.* **1925**, *10*, 22−128.

(2) Susi, T.; Meyer, J. C.; Kotakoski, J. Quantifying transmission electron microscopy irradiation effects using two-dimensional materials. *Nat. Rev. Phys.* **2019**, *1*, 397−405.

(3) Egerton, R. F.; Li, P.; Malac, M. Radiation damage in the TEM and SEM. *Micron* **2004**, *35*, 399−409.

(4) Egerton, R. F. Control of radiation damage in the TEM. *Ultramicroscopy* **2013**, *127*, 100−108.

(5) Jiang, N. Electron beam damage in oxides: A review. *Rep. Prog. Phys.* **2016**, *79*, 016501.

(6) Ugurlu, O.; Haus, J.; Gunawan, A. A.; Thomas, M. G.; Maheshwari, S.; Tsapatsis, M.; Mkhoyan, K. A. Radiolysis to knock-on damage transition in zeolites under electron beam irradiation. *Phys. Rev. B: Condens. Matter Mater. Phys.* **2011**, *83*, 113408.

(7) Komsa, H.-P.; Kotakoski, J.; Kurasch, S.; Lehtinen, O.; Kaiser, U.; Krasheninnikov, A. V. Two-Dimensional Transition Metal Dichalcogenides under Electron Irradiation: Defect Production and Doping. *Phys. Rev. Lett.* **2012**, *109*, 35503.

(8) Wei, X.; Tang, D.-M.; Chen, Q.; Bando, Y.; Golberg, D. Local Coulomb Explosion of Boron Nitride Nanotubes under Electron Beam Irradiation. *ACS Nano* **2013**, *7*, 3491−3497.

(9) Meyer, J. C.; Eder, F.; Kurasch, S.; Skakalova, V.; Kotakoski, J.; Park, H. J.; Roth, S.; Chuvilin, A.; Eyhusen, S.; Benner, G.; et al. Accurate measurement of electron beam induced displacement cross sections for single-layer graphene. *Phys. Rev. Lett.* **2012**, *108*, 196102.

(10) Sommer, B.; Sonntag, J.; Ganczarczyk, A.; Braam, D.; Prinz, G.; Lorke, A.; Geller, M. Electron-beam induced nano-etching of suspended graphene. *Sci. Rep.* **2015**, *5*, 7781.

(11) Egerton, R. F. Choice of operating voltage for a transmission electron microscope. *Ultramicroscopy* **2014**, *145*, 85−93.

(12) Linck, M.; Hartel, P.; Uhlemann, S.; Kahl, F.; Müller, H.; Zach, J.; Haider, M.; Niestadt, M.; Bischoff, M.; Biskupek, J.; et al. Chromatic Aberration Correction for Atomic Resolution TEM Imaging from 20 to 80 kV. *Phys. Rev. Lett.* **2016**, *117*, 076101.

(13) Rose, H. Outline of a spherically corrected semi-aplanatic medium-voltage TEM. *Optik* **1990**, *85*, 19−24.

(14) Haider, M.; Uhlemann, S.; Schwan, E.; Rose, H.; Kabius, B.; Urban, K. Electron microscopy image enhanced. *Nature* **1998**, *392*, 768−769.

(15) Krivanek, O. L.; Dellby, N.; Lupini, A. R. Towards sub-Å electron beams. *Ultramicroscopy* **1999**, *78*, 1−11.

(16) Erni, R.; Rossell, M. D.; Kisielowski, C.; Dahmen, U. Atomic-Resolution Imaging with a Sub-50-pm Electron Probe. *Phys. Rev. Lett.* **2009**, *102*, 096101.

(17) Novoselov, K. S.; Jiang, D.; Schedin, F.; Booth, T. J.; Khotkevich, V. V.; Morozov, S. V.; Geim, A. K. Two-dimensional atomic crystals. *Proc. Natl. Acad. Sci. U. S. A.* **2005**, *102*, 10451−3.

(18) Zhao, X.; Kotakoski, J.; Meyer, J. C.; Sutter, E.; Sutter, P.; Krasheninnikov, A. V.; Kaiser, U.; Zhou, W. Engineering and modifying two-dimensional materials by electron beams. *MRS Bull.* **2017**, *42*, 667−676.

(19) Lehnert, T.; Lehtinen, O.; Algara-Siller, G.; Kaiser, U. Electron radiation damage mechanisms in 2D MoSe2. *Appl. Phys. Lett.* **2017**, *110*, 033106.

(20) Lin, Y. C.; Björkman, T.; Komsa, H. P.; Teng, P. Y.; Yeh, C. H.; Huang, F. S.; Lin, K. H.; Jadczak, J.; Huang, Y. S.; Chiu, P. W.; et al. Three-fold rotational defects in two-dimensional transition metal dichalcogenides. *Nat. Commun.* **2015**, *6*, 6736.

(21) Zhou, W.; Zou, X.; Najmaei, S.; Liu, Z.; Shi, Y.; Kong, J.; Lou, J.; Ajayan, P. M.; Yakobson, B. I.; Idrobo, J.-C. Intrinsic Structural Defects in Monolayer Molybdenum Disulfide. *Nano Lett.* **2013**, *13*, 2615−2622.

(22) Wang, S.; Lee, G.-D.; Lee, S.; Yoon, E.; Warner, J. Detailed Atomic Reconstruction of Extended Line Defects in Monolayer MoS 2. *ACS Nano* **2016**, *10*, 5419−5430.

(23) Lin, J.; Pantelides, S. T.; Zhou, W. Vacancy-Induced Formation and Growth of Inversion Domains in Transition-Metal Dichalcogenide Monolayer. *ACS Nano* **2015**, *9*, 5189−5197.

(24) Fink, R. W.; Jopson, R. C.; Mark, H.; Swift, C. D. Atomic Fluorescence Yields. *Rev. Mod. Phys.* **1966**, *38*, 513−540.

(25) Yoshimura, A.; Lamparski, M.; Kharche, N.; Meunier, V. First-principles simulation of local response in transition metal dichalcogenides under electron irradiation. *Nanoscale* **2018**, *10*, 2388−2397.
(26) Enkovaara, J.; et al. Electronic structure calculations with GPAW: a real-space implementation of the projector augmented-wave method. *J. Phys.: Condens. Matter* **2010**, *22*, 253202.
(27) Doltsinis, N. L.; Marx, D. First Principles Molecular Dynamics Involving Excited States and Nonadiabatic Transitions. *J. Theor. Comput. Chem.* **2002**, *1*, 319−349.
(28) Krasheninnikov, A.; Miyamoto, Y.; Tománek, D. Role of electronic excitations in ion collisions with carbon nanostructures. *Phys. Rev. Lett.* **2007**, *99*, 16104.
(29) Ojanpera, A.; Krasheninnikov, A. V.; Puska, M. Electronic stopping power from first-principles calculations with account for core electron excitations and projectile ionization. *Phys. Rev. B: Condens. Matter Mater. Phys.* **2014**, *89*, 035120.
(30) Zeb, M. A.; Kohanoff, J.; Sánchez-Portal, D.; Arnau, A.; Juaristi, J. I.; Artacho, E. Electronic Stopping Power in Gold: The Role of d Electrons and the H/He Anomaly. *Phys. Rev. Lett.* **2012**, *108*, 225504.
(31) Lee, C.-w.; Schleife, A. Hot-Electron-Mediated Ion Diffusion in Semiconductors for Ion-Beam Nanostructuring. *Nano Lett.* **2019**, *19*, 3939−3947.
(32) Perdew, J. P.; Burke, K.; Ernzerhof, M. Generalized Gradient Approximation Made Simple. *Phys. Rev. Lett.* **1996**, *77*, 3865−3868.
(33) Blöchl, P. E. Projector augmented-wave method. *Phys. Rev. B: Condens. Matter Mater. Phys.* **1994**, *50*, 17953−17979.
(34) Kresse, G.; Hafner, J. Ab initio molecular dynamics for liquid metals. *Phys. Rev. B: Condens. Matter Mater. Phys.* **1993**, *47*, 558−561.
(35) Kresse, G.; Furthmüller, J. Efficiency of ab-initio total energy calculations for metals and semiconductors using a plane-wave basis set. *Comput. Mater. Sci.* **1996**, *6*, 15−50.
(36) Lingerfelt, D. B.; Ganesh, P.; Jakowski, J.; Sumpter, B. G. Electronically Nonadiabatic Structural Transformations Promoted by Electron Beams. *Adv. Funct. Mater.* **2019**, *29*, 1901901.
(37) Lingerfelt, D. B.; Ganesh, P.; Jakowski, J.; Sumpter, B. G. Understanding Beam Induced Electronic Excitations in Materials. *ChemRxiv*, August 20, 2019, ver. 5. DOI: 10.26434/chemrxiv.7726139.v5.
(38) Murphy, N. C.; Wortis, R.; Atkinson, W. A. Generalized inverse participation ratio as a possible measure of localization for interacting systems. *Phys. Rev. B: Condens. Matter Mater. Phys.* **2011**, *83*, 184206.
(39) Parkin, W. M.; Balan, A.; Liang, L.; Das, P. M.; Lamparski, M.; Naylor, C. H.; Rodríguez-Manzo, J. A.; Johnson, A. T.; Meunier, V.; Drndić, M. Raman Shifts in Electron-Irradiated Monolayer MoS_2. *ACS Nano* **2016**, *10*, 4134−4142.
(40) McKinley, W. A.; Feshbach, H. The Coulomb Scattering of Relativistic Electrons by Nuclei. *Phys. Rev.* **1948**, *74*, 1759−1763.
(41) Bethe, H. Theorie des Durchgangs schneller Korpuskular-strahlen durch Materie. *Ann. Phys.* **1930**, *397*, 325−400.
(42) Inokuti, M.; Kim, Y.-K.; Platzman, R. L. Total Cross Sections for Inelastic Scattering of Charged Particles by Atoms and Molecules. I. A Sum Rule for the Bethe Cross Sections and Its Application to the Helium Atom. *Phys. Rev.* **1967**, *164*, 55−61.
(43) Docherty, C. J.; Parkinson, P.; Joyce, H. J.; Chiu, M. H.; Chen, C. H.; Lee, M. Y.; Li, L. J.; Herz, L. M.; Johnston, M. B. Ultrafast transient terahertz conductivity of monolayer $MoS_2$and WSe2 grown by chemical vapor deposition. *ACS Nano* **2014**, *8*, 11147−11153.
(44) Li, L.; Long, R.; Bertolini, T.; Prezhdo, O. V. Sulfur Adatom and Vacancy Accelerate Charge Recombination in MoS 2 but by Different Mechanisms: Time-Domain Ab Initio Analysis. *Nano Lett.* **2017**, *17*, 7962−7967.

https://dx.doi.org/10.1021/acs.nanolett.0c00670
Nano Lett. 2020, 20, 2865−2870